JGR Biogeosciences

RESEARCH ARTICLE
10.1029/2019JG005293

Carbon Dioxide Fluxes to the Atmosphere From Waters Within Flooded Forests in the Amazon Basin

Joao Henrique Fernandes Amaral[1,2], John M. Melack[1], Pedro Maia Barbosa[1], Sally MacIntyre[1], Daniele Kasper[3], Alicia Cortés[1], Thiago Sanna Freire Silva[4], Rodrigo Nunes de Sousa[2], and Bruce R. Forsberg[2]

[1]Earth Research Institute, University of California, Santa BarbaraCalifornia, [2]Laboratório de Ecossistemas Aquáticos, Instituto Nacional de Pesquisas da Amazônia, Manaus, Amazonas, Brazil, [3]Instituto de Biofísica Carlos Chagas Filho, Universidade Federal do Rio de Janeiro, Rio de JaneiroRio de Janeiro, Brazil, [4]Biological and Environmental Sciences, Faculty of Natural Sciences, University of Stirling, Stirling, UK

Key Points:
- CO_2 concentrations in near-surface waters within flooded Amazon forests ranged from 19 to 329 μM and CO_2 fluxes from −0.8 to 55 mmol m^{-2} hr^{-1}
- Daytime CO_2 fluxes were higher at a wind-protected site, while night-time fluxes were often higher at a wind-exposed site
- On an areal basis, CO_2 fluxes from flooded forests during high water levels are the major contributor among aquatic habitats

Supporting Information:
- Supporting Information S1

Correspondence to:
J. H. F. Amaral,
jh.amaral@gmail.com

Citation:
Amaral, J. H. F., Melack, J. M., Barbosa, P. M., MacIntyre, S., Kasper, D., Cortés, A., et al. (2020). Carbon dioxide fluxes to the atmosphere from waters within flooded forests in the Amazon basin. *Journal of Geophysical Research: Biogeosciences*, *125*, e2019JG005293. https://doi.org/10.1029/2019JG005293

Received 3 JUN 2019
Accepted 15 JAN 2020
Accepted article online 21 JAN 2020

Author Contributions:
Conceptualization: Joao Henrique Fernandes Amaral, John M. Melack, Pedro Maia Barbosa, Sally MacIntyre, Alicia Cortés, Bruce R. Forsberg
Formal analysis: Joao Henrique Fernandes Amaral, Pedro Maia Barbosa, Sally MacIntyre, Daniele Kasper, Alicia Cortés, Thiago Sanna Freire Silva, Rodrigo Nunes de Sousa
Funding acquisition: John M. Melack, Pedro Maia Barbosa, Bruce R. Forsberg
Investigation: Joao Henrique Fernandes Amaral, Bruce R. Forsberg
Methodology: Joao Henrique Fernandes Amaral, John M. Melack, Pedro Maia Barbosa, Daniele Kasper, Alicia Cortés
Project administration: Joao Henrique Fernandes Amaral, John M.
(continued)

Abstract Inundated tropical forests are underrepresented in analyses of the global carbon cycle and constitute 80% of the surface area of aquatic environments in the lowland Amazon basin. Diel variations in CO_2 concentrations and exchanges with the atmosphere were investigated from August 2014 to September 2016 in two flooded forests sites with different wind exposure within the central Amazon floodplain (3°23′S, 60°18′W). CO_2 profiles and estimates of air–water gas exchange were combined with ancillary environmental measurements. Surface CO_2 concentrations ranged from 19 to 329 μM, CO_2 fluxes ranged from −0.8 to 55 mmol m^{-2} hr^{-1} and gas transfer velocities ranged from 0.2 to 17 cm hr^{-1}. CO_2 concentrations and fluxes were highest during the high water period. CO_2 fluxes were three times higher at a site with more wind exposure (WE) compared to one with less exposure (WP). Emissions were higher at the WP site during the day, whereas they were higher at night at the WE site due to vertical mixing. CO_2 concentrations and fluxes were lower at the W P site following an extended period of exceptionally low water. The CO_2 flux from the water in the flooded forest was about half of the net primary production of the forest estimated from the literature. Mean daily fluxes measured in our study (182 ± 247 mmol $m^{-2}d^{-1}$) are higher than or similar to the few other measurements in waters within tropical and subtropical flooded forests and highlight the importance of flooded forests in carbon budgets.

Plain Language Summary Aquatic habitats in the lowland Amazon emit large quantities of carbon dioxide (CO_2). However, information on CO_2 fluxes from seasonally flooded forests that constitute 80% of the surface area of aquatic environments in the lowland Amazon basin is sparse. We provide the first multi-year measurements of CO_2 exchanges within flooded forests of the central Amazon basin. Our approach combines measurement of dissolved CO_2 concentrations and fluxes between the water and atmosphere and ecological data. Although the rates of CO_2 emission by flooded forests are lower than other aquatic habitats, such as open waters in rivers and lakes, the combination of high CO_2 concentrations and a large area results in an appreciable regional out gassing of carbon dioxide from flooded forests. These fluxes can represent about half of the net primary production of flooded forests in the central Amazon basin.

1. Introduction

Recent syntheses of carbon processing and evasion to the atmosphere from inland aquatic ecosystems have revealed the disproportionately large contribution, relative to their area, that these ecosystems make to carbon cycling and the importance of outgassing of carbon dioxide (Cole et al., 2007; Lehner & Döll, 2004; Raymond et al., 2013). Tropical freshwater systems are underrepresented in these analyses, and seasonally, inundated forests are seldom considered. Within the lowland Amazon basin, seasonally inundated and riparian forests cover approximately 750,000 km^2, 15% of the whole lowland area, and are important to the ecology and biogeochemistry of the region (Junk et al., 2010; Melack & Hess, 2010). Floodplain forests occur in an aquatic terrestrial transition zone (ATTZ; Junk et al., 1989) and are inundated for varying portions of the year depending on water level and local topography (Wittmann et al., 2010). Inundated forests and other floodplain habitats add organic carbon and dissolved CO_2 to floodplains and rivers (Melack & Engle, 2009; Melack & Forsberg, 2001; Worbes, 1997) and contribute to evasion of CO_2 and methane from

Melack, Pedro Maia Barbosa, Bruce R. Forsberg
Resources: John M. Melack, Pedro Maia Barbosa, Bruce R. Forsberg
Software: Alicia Cortés, Thiago Sanna Freire Silva, Rodrigo Nunes de Sousa
Supervision: John M. Melack, Pedro Maia Barbosa, Bruce R. Forsberg
Writing - original draft: Joao Henrique Fernandes Amaral, John M. Melack, Pedro Maia Barbosa, Sally MacIntyre, Daniele Kasper, Alicia Cortés, Bruce R. Forsberg
Writing – review & editing: Daniele Kasper

these aquatic environments (Abril et al., 2014; Melack, 2016; Melack et al., 2004; Pangala et al., 2017; Richey et al., 2002). However, almost all studies of CO_2 outgassing from Amazon floodplains have been restricted to open water areas.

CO_2 exchanges with the atmosphere are determined by the gradient of water–air CO_2 concentrations and by the gas transfer velocity (k), a function of turbulence at the air–water interface (MacIntyre et al., 1995; Zappa et al., 2007). Most computations of carbon fluxes from lakes and wetlands use simple wind-based equations of k, though other mechanisms are recognized as important in tropical, temperate, and arctic lakes (MacIntyre et al., 2002; MacIntyre et al., 2018; MacIntyre & Melack, 1995; Tedford et al., 2014), as well as wetlands (Poindexter et al., 2016). Vegetated aquatic habitats, such as flooded forests, are likely to experience lower wind speeds than open water areas. However, diel variations in cooling or heating of surface waters and associated horizontal water motions and convective mixing can enhance gas exchange even at low wind speeds (MacIntyre et al., 2019). Direct measurements of k, water–air CO_2 concentration gradients, and meteorological parameters in flooded forests are needed to better understand the mechanisms associated with CO_2 outgassing from these aquatic habitats and to evaluate their role in the carbon cycle.

The first regional estimate of CO_2 outgassing for the aquatic habitats of the Amazon basin (Richey et al., 2002) reported CO_2 outgassing of 830 ± 240 Mg C·km^{-2} yr^{-1}. Subsequent measurements conducted in lakes (Polsenaere et al., 2013; Rudorff et al., 2011), reservoirs (Kemenes et al., 2011), and rivers (Alin et al., 2011; de Rasera et al., 2013; Sawakuchi et al., 2017) reported higher k values compared to the values used by Richey et al. (2002). Although seasonally flooded forests can cover large areas, data on k and CO_2 concentrations and fluxes in these habitats are lacking and likely are different from the conditions in the lakes, reservoirs, and rivers.

Our study contributes to understanding of Amazon floodplains and regional carbon cycling. We provide new information on CO_2 dynamics in inundated forests, the largest aquatic habitat in the Amazon basin, but the one least studied. We report CO_2 concentrations, evasion rates, and gas transfer velocities measured in flooded forests fringing a floodplain lake along the Solimões River as function of seasonal changes in water depth and day to night differences over the course of two distinct hydrological years. Contrasting exposure to wind is considered in our analysis, and we test the following hypotheses: (1) The proximity and the extent of open water areas close to flooded forest sites will lead to different CO_2 fluxes in the forests. (2) Wind-protected forests will have lower k values and consequently lower CO_2 fluxes than wind-exposed sites. (3) Flooded forests have high rates of CO_2 evasion to the atmosphere and make a large contribution to regional CO_2 evasion in the Amazon basin.

2. Methods

2.1. Site Description and Sampling

Measurements over 2 years were made in two contrasting flooded forest sites in Lake Janauacá (3°23′S, 60°18′W; altitude 32 m), located on the southern side of the Solimões River in the central Amazon basin (Figure 1). The sites differed in wind exposure and fetch of adjacent open water areas and are called wind-exposed flooded forest (WE; 3°23′19.0″S, 60°15′14.8″W) and wind-protected flooded forest (WP; 3°24′20.6″S, 60°14′48.8″W). The WP site is in an embayment with a fetch of 50 to 100 m for typical wind directions. The WE site is located on the edge of the main lake and had a fetch varying from 1 to 4 km depending on wind direction and water level.

The forests investigated are influenced by sediment and nutrient rich water from the Solimões River and are called *várzea* forests (Wittmann et al., 2002). Trees on these floodplains respond phenologically, morphologically, and physiologically to periodic flooding that varies as a function of the water level of the Solimões River and the topography of the ATTZ (Parolin et al., 2010; Worbes, 1997). Phenological behavior is largely associated with the time and extent of inundation, and evergreen, semideciduous, and deciduous species shred their leaves at different times (Parolin et al., 2010). *Piranhea trifoliata* and *Vitex cymosa* are common tree species (Worbes et al., 1992). The Janauacá floodplain and nearby systems have been the focus of prior studies of hydrology and limnology (Bonnet et al., 2017; Melack et al., 2009; Melack & Forsberg, 2001).

Measurements of carbon dioxide partial pressure (pCO_2) and CO_2 emissions were made when the sites were flooded and accessible at multiple times of the day and night. Measurements were made on 12 occasions

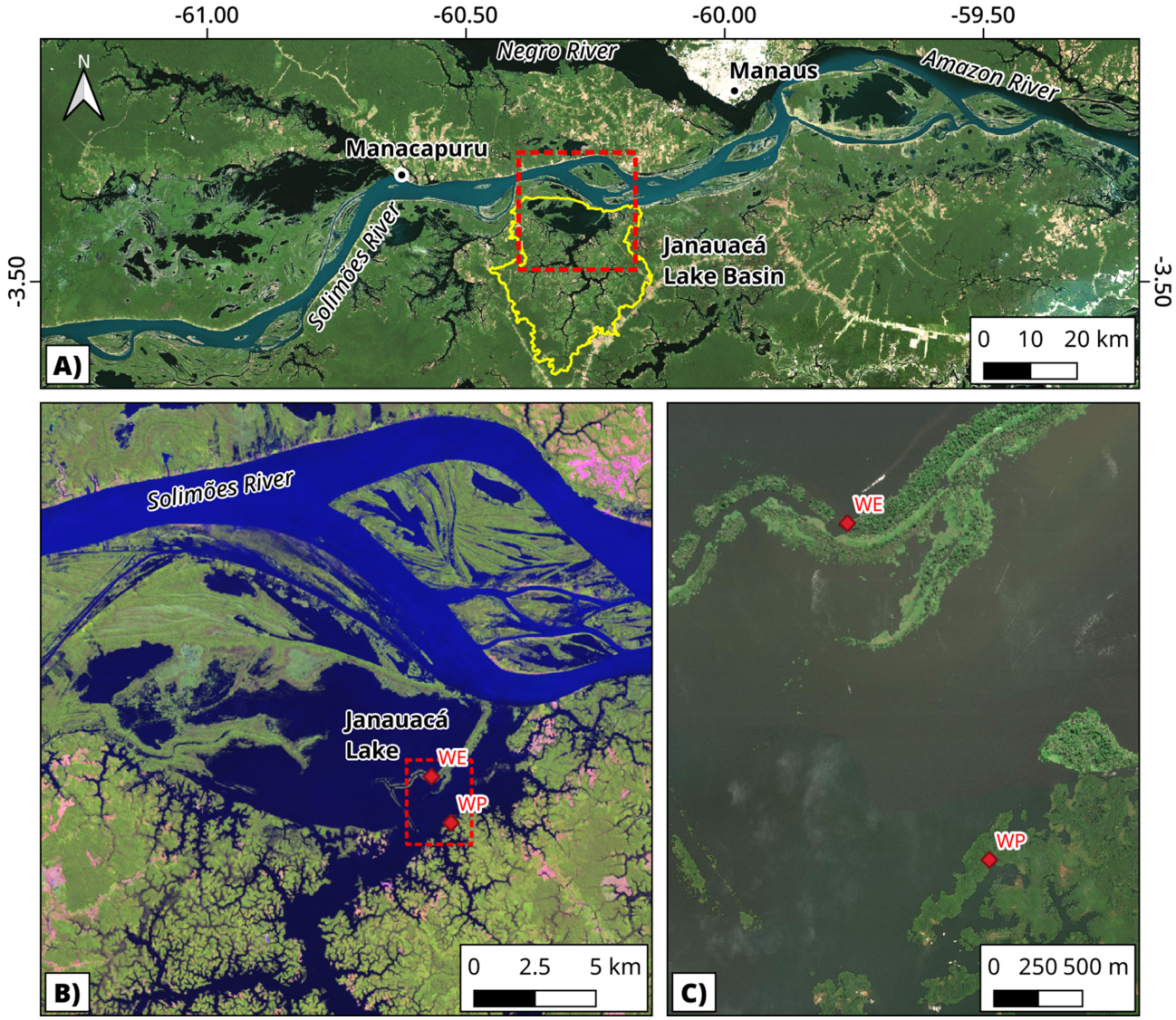

Figure 1. (a) General location of the study site showing the watershed (yellow line; Background: ESRI World Imagery). (b) Composite high-water Landsat 8 image showing the upper Janauacá floodplain (red dashed). (c) Location of the sampled flooded forest sites: wind-exposed site (WE) and wind-protected site (WP). Red dashed lines indicate the boundaries of the following figure panel. Janauacá lake basin delimited by Pinel et al. (2015).

between August 2014 and September 2016, representing different hydrological phases. The following periods were sampled: August 2014 (falling water—FW), February to April 2015 (rising water—RW), May to July 2015 (high water—HW), August 2015 (FW), September 2015 (FW), July 2016 (HW), and August and September 2016 (FW). The WP site was sampled in all campaigns, while the WE site only in 2015 (Figure S1 in the supporting information).

2.2. Analytical Methods

pCO_2 was measured with an off-axis integrated cavity output spectrometer (Ultraportable Greenhouse Gas Analyzer, Los Gatos Research) connected to a marble-type equilibrator (Frankignoulle et al., 2001), through which water from different depths was pumped (3 L min^{-1}). CO_2 fluxes across the air–water interface were measured using floating chambers connected in a closed loop to the Ultraportable Greenhouse Gas Analyzer. All measurements were made in replicate as ~10-min deployments from a moored boat. The chambers had an internal volume of 15 L and an internal area of 0.11 m^2. Fluxes were calculated from the slope of partial pressure versus time, which was linear with r^2 greater than 0.9. The detection limit of our fluxes measurements was calculated as 0.22 mmol m^{-2} hr^{-1} of CO_2. Further details of the

equilibrator setup and gas analyzer accuracy are given in Amaral et al. (2018) and for the chamber design in Barbosa et al. (2016).

We estimated gas transfer velocity (k) from the formulation $F = k[\Delta CO_2]$ using our measurements of CO_2 fluxes (F) and the difference between observed and equilibrium gas concentrations (ΔCO_2) derived from the pCO_2 measurements in water and air and using Henry's constant. To estimate the gas concentrations in water and air, we first corrected the dry air in the instrument to wet air using the water vapor computed from temperature measured at lake surface (Weiss & Price, 1980), and then used the Henry's constant for CO_2 from Wiesenburg and Guinasso (1979) to calculate concentration. Estimated k values were normalized to 20 °C (k_{600}) for which 600 is the Schmidt number for CO_2 at 20 °C and Sc at other temperatures were obtained from Wanninkhof (1992).

Near-surface pH (Orion Star, Thermo Scientific; precision of 0.1, calibrated with 4.0, and 7.0 standards), maximum depth measured with a weighted graduated line, and depth profiles of conductivity and temperature measured with a profiler (Castway, Sontek Inst. Co) at 0.3 m intervals were obtained during each sampling period. Time series measurements of temperature and dissolved oxygen (DO) were obtained at each site using thermistors with 0.002 °C accuracy (RBRsolo) recording every 0.5 s, and with optical DO sensors (PME MiniDOT loggers) recording every 10 min (accuracy of 5% of measurement or 0.3 mg L^{-1}, whichever is larger, and resolution of 0.01 mg L^{-1}). Wind speed and direction sensors (Onset, Inc.) were deployed at a height of 2 m on a floating buoy at open water sites close to flooded forest sites. Average wind speeds were calculated for the hour before the flux measurements.

Samples from ~0.3 m for chlorophyll (Chl-a), dissolved organic carbon (DOC), total suspended solids (TSS), total nitrogen (TN), and total phosphorus (TP) analyses were collected once on each campaign at both stations. Chl-a samples were filtered through glass fiber GF/F filters (Whatman) and kept frozen in the dark until analysis. Chl-a was determined spectrophotometrically, following filter maceration and extraction in 90% acetone, using the trichromatic equations of Strickland and Parsons (1972). TSS was determined by weighing particulates collected on pre-weighed Millipore HA filters (0.45 μm pore size), following the method of Kasper et al. (2018). DOC samples were filtered through pre-combusted (450–500 °C for 1 hr) glass fiber GF/F filters (Whatman), collected in pre-cleaned (10% HCl wash, deionized water rinse) and pre-combusted (450–500 °C for 1 hr) borosilicate vials, and then stored at 4 °C until analysis. DOC was determined using a total organic carbon analyzer (TOC-V Shimadzu). TN and TP were determined by simultaneous analysis on unfiltered samples after persulfate digestion (Valderrama, 1981) followed by nitrate and phosphorus assays (Strickland & Parsons, 1972).

We estimated flooded forest area for the northern portion of Janauacá for each sampling date using an image classification method to discriminate floodable forest habitats and other land covers and a digital elevation model derived for the lake (Pinel et al., 2015). Forest vegetation (including trees and shrubs) was classified using all bands of a Landsat 8 OLI image acquired in April 2016, when all floodable shrubs and trees were emergent. We used eCognition software to perform multiresolution image segmentation, delineating homogeneous land cover units within the image. We then developed classification rules to discriminate forest and shrub areas based on the Normalized Difference Vegetation Index and the Normalized Difference Water Index (Gao, 1996). We used the digital elevation model and daily observations of water surface elevation, made at a differential GPS calibrated gauging station on the lake (Pinel et al., 2015), to estimate inundated area for each sampling occasion. Finally, we used the classified image together with the inundation maps to estimate the total area of flooded forest for each sampling period.

To account for the influence of forests with different wind exposure on CO_2 fluxes, we separated the flooded forest into two categories: (1) sheltered flooded forest (WP), representative of flooded forests at the WP site, and (2) WE, similar to that found at the WE site. To define the WE forest area, we delimited the perimeter of the largest open water area in the lake and then selected a 100 m band of forest immediately adjacent to this region. All remaining flooded forest was defined as WP. All analyses were done with ArcGIS version 11.0 (ESRI, Inc.).

To combine measurements of fluxes and estimates inundated forest areas to calculate annual fluxes (F, Gg C yr^{-1}) from the flooded forests in the northern region of Janauacá, an expression similar to that in Melack et al. (2004) was used:

$$F = \sum_{j=1}^{2} \sum_{i=1}^{8} \left(f_{ij} \cdot A_{ij} \cdot t \right),$$

f is the mean daily flux of CO_2 for each month and site (g C·m^{-2} d^{-1}), A is flooded forest area for each month (km^2), t is the number of days per month, i is the index for each month (from February to September), and j is the index for each site (WP and WE).

To estimate the uncertainty of the estimates, we conducted a Monte Carlo error analysis using the measurements obtained each month and for data lumped into RW, HW, and FW periods. To do so, we randomly resampled with repetition the measurements for each period to create 100 artificial data and computed the arithmetic mean (m) and standard deviation (std) of these data using the *bootstrp* function in Matlab. We then computed the maximum likelihood estimators as MLE = exp($m + std^2/2$) and 95% confidence intervals (CI; Dixon, 1993).

2.3. Statistical Analyses

CO_2 concentration, k_{600}, and CO_2 fluxes were compared between WP and WE sites for only the first year as WE sites were not accessible in the second year. Tests for normality and homoscedasticity indicated that CO_2 concentrations were normally distributed, but k_{600} and CO_2 fluxes were not unless log transformed. Parametric tests were used in all comparisons, using log transformed data, as required. The student t test was used for comparisons between WP and WE sites. A one-way analysis of variance (ANOVA) followed by post hoc pair-wise t tests, with correction for multiple tests done by the Benjamin–Hochberg method, was used to compare hydrological periods. We separated measurements conducted over 24 hr into categories of day (6:00 a.m. to 6:00 p.m.) and night (6:00 p.m. to 6:00 a.m.) to evaluate the implications of sampling time for CO_2 fluxes, variability of k_{600}, and CO_2 concentrations. We compared day and night values using all data and data separated by site by paired t test.

To assess the potential influences of environmental variables on CO_2 concentrations measured in flooded forests with contrasting wind exposure, we applied a multimodel selection and averaging approach (Grueber et al., 2011) of linear mixed-effects models with maximum likelihood using the *lme4* package in R. The model was structured with CO_2 concentration as a response variable, site (WP and WE) as random factors, and the total area of flooded forest for each sampling period, surface temperature, TSS, DO, TN, TP, DOC, and Chl-*a* as fixed variables. We generated and evaluated the small-sample corrected Akaike information criterion (AICc), ΔAICc, and AICc model weights (wi) using the *dredge* function within the *MuMIn* package (Barton & Barton, 2018). The final model sets were simplified from all possible models by retaining only the top models within two units of ΔAICc of the "best" model. We calculated a daily geometric mean of CO_2 concentration for each site and sampling occasion and used these values in the models, as we made only one measurement in each campaign for some environmental predictors: Chl-*a*, TP, TN, DOC, and TSS. Before model selection, we first tested for outliers among explanatory variables (one exclusion was made). Second, we identified and excluded from the full model colinear predictors. For these steps, we use the outlierTest and vif function, respectively, both within the package car (Fox et al., 2012).

To estimate parameter coefficients in the final model set, we calculated conditional values using the mean of regression coefficients weighted by the AICc weight (wi) from each model including that variable (Burnham & Anderson, 2002). Predictor relative importance or variable weights were calculated for each term in the models via the natural average method for the coefficients, that is, by summing the weights of models where each variable appears (Galipaud et al., 2014; Grueber et al., 2011). Using z tests, individual parameters in model-averaged sets were tested for statistical significance as the deviation of coefficients from zero. Parametric assumptions of linear models were verified using plots of residuals for normality and homoscedasticity. Statistical analyses and graphics were done with R Studio Version 1.1.456.

3. Results

3.1. CO_2 Concentrations and Fluxes

Surface CO_2 concentrations ranged from 19 to 329 μM (pCO_2 = 664 to 11,006 μatm); the overall geometric mean was 134 μM, and the mean and standard deviation were 155 ± 71 μM (pCO_2 = 4,465; 5,117 ± 2,326 μatm; Table 1). One hundred seventy measurements of CO_2 flux were made at the two

Table 1
Near-surface CO_2 Concentrations, Flux and Gas Transfer Velocities (k_{600}) Measured in Wind-exposed (WE) and Wind-protected (WP) Flooded Forests

		CO_2 (μM)		CO_2 flux (mmol m^{-2} hr^{-1})		K_{600} (cm hr^{-1})	
		WP	WE	WP	WE	WP	WE
Period	Month	Mean, *SD* (min/max, n)	Mean, *SD* (min/max, n)	Mean, *SD* (min/max, n)	Mean, *SD* (min/max, n)	Mean, *SD* (min/max, n)	Mean, *SD* (min/max, n)
Falling water	Aug 2014	158 ± 43 (112/216, 5)		2.8 ± 1.2 (0.9/4.6,13)		1.5 ± 0.7 (0.4/2.6, 13)	
Rising water	Feb 2015	166 ± 53 (106/244, 5)	61 ± 37 (19/89, 3)	5.2 ± 3.2 (0.5/10.1, 13)	1.4 ± 1.8 (−0.8[a] /3.9, 5)	2.5 ± 1.1 (0.3/4.2, 13)	4.1 ± 2.5 (1.7/8.0, 5)
	March 2015	90 ± 17 (81/110, 3)	100 ± 16 (87/118, 3)	3.4 ± 2.1 (1.6/5.7, 3)	3.2 ± 1.0 (2.3/4.3, 3)	3.3 ± 1.4 (1.8/4.5, 3)	2.9 ± 1.1 (1.8/4, 3)
	April 2015	156 ± 24 (137/184, 3)	237 ± 19 (226/259, 3)	8.5 ± 5.8 (3.4/14.6, 4)	17 ± 4.0 (11/22, 6)	5.3 ± 4.0 (1.8/9.5, 4)	6.4 ± 1.8 (3.7/8.3, 6)
High water	May 2015	202 ± 17 (186/221, 3)	236 ± 15 (219/246, 3)	7.7 ± 1.7 (5.4/10.5, 6)	36 ± 10 (18/48, 7)	3.2 ± 0.6 (2.3/4, 6)	12.8 ± 3.5 (6.8/16.8, 7)
	June 2015	217 ± 27 (189/243, 3)	227 ± 57 (177/289, 3)	6.9 ± 4.9 (4.4/16.7, 6)	30 ± 19 (13/55, 6)	2.6 ± 1.8 (1.6/6.2, 6)	10 ± 4.8 (4.9/16, 6)
	July 2015	190 ± 7 (182/196, 3)	187 ± 14 (174/202, 3)	4.6 ± 2.6 (1.7/9.1, 6)	30 ± 8.5 (13/33, 6)	2.1 ± 1.2 (0.8/4.2, 6)	9.7 ± 4.2 (5.6/15, 6)
Falling water	Aug 2015	265 ± 70 (177/329,4)	180 ± 22 (163/213, 4)	5.4 ± 2.5 (2.7/9.7, 10)	16 ± 8.3 (8/31, 8)	1.6 ± 1.1 (0.7/4.3, 10)	7.4 ± 4.7 (2.9/16, 8)
	Sept 2015	157 ± 66 (83/244, 4)	172 ± 49 (123/250, 5)	2.6 ± 1.8 (1.4/7.3, 9)	6 ± 2.1 (3/10, 17)	2.1 ± 1.9 (0.7/6.9, 9)	3.3 ± 2.3 (1.3/8.3, 17)
High water	July 2016	111 ± 36 (80/164, 5)		3.6 ± 1.2 (2.1/5.4, 10)		3.1 ± 1.6 (1.8/5.9, 10)	
Falling water	Aug 2016	55 ± 13 (41/70, 5)		1.0 ± 0.3 (0.5/1.3, 11)		1.7 ± 0.3 (1.4/2.3, 11)	
	Sept 2016	94 ± 66 (24/203, 10)		1.7 ± 1.3 (0.1/4.8, 21)		1.9 ± 1.4 (0.2/6, 21)	

Note. *SD* is the standard deviation; min/max indicates the minimum and maximum values among the n measurements on each date.
[a]The ingassing value was measured when Chl-*a* concentrations were high (18 μg L^{-1} in the flooded forest and 25 μg L^{-1} in associated open water), suggesting that Chl-*a* enriched water was advected from the open water into the flooded forest site. One replicate measurement was negative, and one was positive; both had high r^2 (>0.95). When replicates were averaged, the value was slightly negative.

flooded forests sites, and fluxes ranged from −0.8 to 55 mmol m^{-2} hr^{-1} with an overall mean and standard deviation of 7.8 ± 10.1 mmol m^{-2} hr^{-1} (Table 1). Gas transfer velocities derived from these measurements ranged from 0.2 to 17 cm hr^{-1} with an overall geometric mean value of 2.6 cm hr^{-1} and mean and standard deviation of 3.8 ± 3.6 cm hr^{-1} (Table 1). Mean CO_2 concentrations were similar at the two sites (WE, 175 ± 65 μM and WP, 178 ± 60 μM; Welch two sample *t* test, $t(58) = 0.2$, $p = 0.84$; Figure 2). CO_2 fluxes and k_{600} were greater at the WE site (16 ± 14 mmol m^{-2} hr^{-1} and 6.7 ± 4.6 cm hr^{-1}) compared to the WP site (5 ± 3 mmol m^{-2} hr^{-1} and 2.4 ± 1.7 cm hr^{-1}) based on Welch two sample *t* test ($t(82) = -5.4$, $p < 0.001$ and $t(112.2) = -7.9$, $p < 0.001$, respectively).

Surface CO_2 concentrations differed seasonally at the WE site based on one-way ANOVA ($F(2,24) = 4.9$, $p = 0.02$). Values were higher during high water (HW; 218 ± 36 μM, $n = 19$) relative to rising water (RW; 143 ± 89 μM, $n = 14$), but similar (pairwise *t* test, $p = 0.14$) to concentrations during FW (173 ± 39 μM, $n = 25$; Figure 2). Seasonal differences also occurred at the WP site ($F(4,48) = 9.9$, $p < 0.001$). In Year 1, the CO_2 concentrations measured at the WP site were higher during HW (203 ± 20 μM, $n = 18$) and FW (193 ± 71 μM, $n = 32$) compared to RW (154 ± 47 μM, $n = 20$; pairwise *t* test, $p = 0.03$ and $p = 0.05$, respectively). In Year 2, no differences were found between HW (81 ± 38 μM, $n = 21$) and FW (96 ± 64 μM, $n = 21$), but mean surface CO_2 concentrations measured in those periods were consistently lower than the values measured in HW and FW periods of the first year of study (pairwise *t* test, $p < 0.001$; Table 1).

CO_2 fluxes and k_{600} for both sites varied with the phase of the hydrological cycle based on one-way ANOVA. At the WE site, CO_2 fluxes ($F(2,55) = 19$, $p < 0.001$) and values of k_{600} ($F(2,55) = 17$, $p < 0.001$) tracked changes in the water level, with greater mean values observed during high water (29 ± 14 mmol m^{-2} hr^{-1} and 11 ± 4 cm hr^{-1}, $n = 19$) relative to rising (9 ± 8 mmol m^{-2} hr^{-1} and 5 ± 2 cm hr^{-1}, $n = 14$) and FW

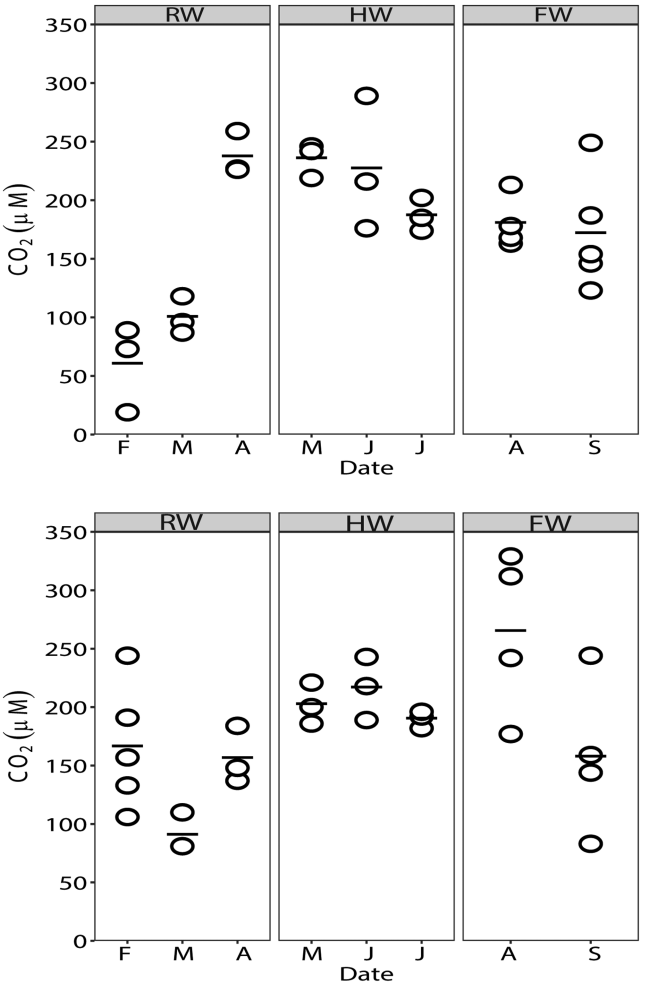

Figure 2. CO_2 concentrations measured at the wind-exposed site (WE, upper panel) and wind-protected site (WP, lower panel) for hydrological phases: rising water (RW), high water (HW) and falling water (FW). Horizontal bars represent the mean per sampling date, open circles represent each observation in a 24 hr period.

(9 ± 7 mmol m^{-2} hr^{-1} and 5 ± 4 cm hr^{-1}, $n = 25$; pairwise t test, $p < 0.001$; Figure 3). At the WP site, mean CO_2 fluxes ($F(4,107) = 16.2$, $p < 0.001$) were also higher during high water (6 ± 3 mmol m^{-2} hr^{-1}, $n = 18$) compared to FW (4 ± 2 mmol m^{-2} hr^{-1}, $n = 32$) but similar to mean values encountered during rising water (6 ± 4 mmol m^{-2} hr^{-1}, $n = 20$) of Year 1 (pairwise t test, $p = 0.001$; Figure 3). Differences in mean k_{600} between periods of the hydrological cycle ($F(4,107) = 4.6$, $p = 0.002$) were higher when comparing the rising water (3 ± 2 cm hr^{-1}, $n = 20$) and high water periods (3 ± 1 cm hr^{-1}, $n = 18$) against the FW period (2 ± 1 cm hr^{-1}, $n = 32$) in Year 1 (pairwise t test, $p = 0.01$ and $p = 0.02$, respectively). In Year 2, mean CO_2 fluxes for a given period of the hydrological cycle were consistently lower than the mean values measured in all periods of Year 1 at the WP site (pairwise t test, $p < 0.001$; Table 1). For k_{600}, the FW period of Year 2 was similar to the FW period of Year 1 (pairwise t test, $p = 0.99$) and also lower than high water (pairwise t test, $p = 0.03$) and rising water periods (pairwise t test, $p = 0.02$) of Year 1 (Table 1).

Day–night differences were statistically different for CO_2 fluxes when comparing all measurements at both sites (paired t test, $t(11) = 3.8$, $p = 0.003$). When differentiating between WP and WE sites, mean CO_2 concentrations were numerically lower during the day (WP = 128 ± 68 μM, $n = 33$, and WE = 166 ± 56 μM, $n = 13$) compared to the night (WP = 172 ± 72 μM, $n = 20$, and WE = 183 ± 74 μM, $n = 14$) at both sites, although they were not statistically different (paired t test, WP: $t(11) = -0.63$, $p = 0.54$; WE: $t(7) = -0.4$, $p = 0.7$). CO_2 fluxes and k_{600} were statistically different only for the WP site. CO_2 fluxes (paired t test, $t(11) = 2.7$, $p = 0.02$) and k_{600} (paired t test, $t(11) = 2.7$, $p = 0.02$) were lower during the night (3.6 ± 2.6 mmol m^{-2} hr^{-1} and 2 ± 0.5 cm hr^{-1}, $n = 42$) compared to the day (3.9 ± 3.3 mmol m^{-2} hr^{-1} and 3 ± 2 cm hr^{-1}, $n = 70$; Figure 4) and consistent with day–night differences at this site for wind speeds that were also higher during the day compared to the night (unpaired t test, $t(51) = 3.5$, $p = 0.0009$). Although not significantly different, we found numerically higher mean values for CO_2 fluxes and k_{600} during the night (20 ± 17 mmol m^{-2} hr^{-1} and 8 ± 5 cm hr^{-1}, $n = 29$) compared to the day (12 ± 9 mmol m^{-2} hr^{-1} and 6 ± 4 cm hr^{-1}, $n = 29$) at the WE site. Wind differences at this site followed the same trend as for the WP site with higher wind speeds during the day (unpaired t test, $t(24) = 2.2$, $p = 0.04$), but the higher fluxes during the night were associated with vertical mixing (Figure 5).

3.2. Environmental Variables and Relationships with CO_2 Concentrations

Environmental variables varied with water level. When depths were low during rising and FW, Chl-*a*, DO, TN, TSS, conductivity, and temperatures were higher compared to high water. Average hourly wind records prior to CO_2 flux measurements varied from below detection to 2.2 m s^{-1} at the WP site and from 0.3 to 5.1 m s^{-1} at the WE site (frequency distributions are given in Figure S2). Environmental variables for both sites are summarized in Table S1.

DO was strongly inversely correlated to CO_2 concentrations ($n = 80$, $r^2 = -0.86$, $p < 0.001$). We identified one outlier among our environmental variables. The outlier was high Chl-*a* and high CO_2 concentrations that occurred at the WP site during the FW in 2015. At that time, the thermocline deepened causing upwelling of nutrient-enriched waters that caused an increase in Chl-*a*, and water enriched in CO_2 concentration was upwelled that raised CO_2 concentrations. DO was the only environmental predictor that was retained from the multimodel selection procedure. It has an AICc value of 149.9 and explained around 90% (marginal R^2) or 97% (conditional R^2) variability in surface CO_2 concentration.

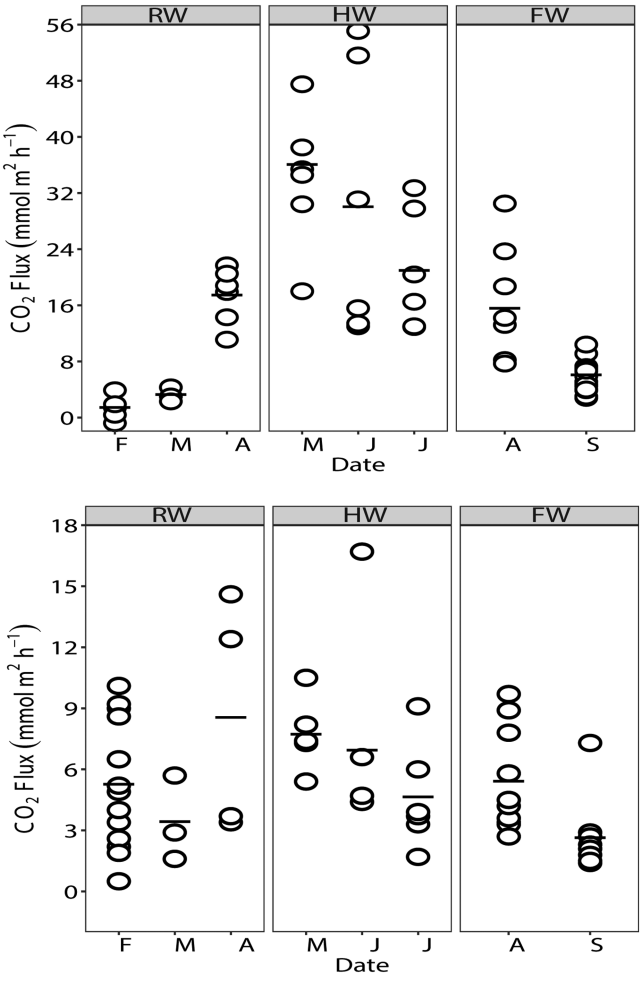

Figure 3. CO_2 evasion measured at the wind-exposed site (WE, upper panel) and wind-protected site (WP, lower panel) for hydrological phases: rising water (RW), high water (HW) and falling water (FW). Horizontal bars represent the mean, open circles represent each observation in a 24 hr period. Note differences in scale of y axis between sites.

3.3. Spatial and Seasonal Integration of CO_2 Fluxes

The WP forests in the northern Janauacá floodplain had a total area of 94 km^2, which corresponds to 88% of the total area of floodable forest estimated for this part of the lake. The remaining 12% is attributed to areas with WE forests.

The maximum likelihood estimator of the flux for all inundated forests in the Janauacá floodplain is 45 Gg·C yr^{-1} with CI of 31 to 69 Gg·C yr^{-1}. Emissions from sheltered forests represent 31 Gg·C yr^{-1} with CI of 21 to 49 Gg·C yr^{-1} and those from wind-exposed forests 14 Gg·C yr^{-1} with CI of 10 to 20 Gg·C yr^{-1}. These values were almost the same based on calculations per month and for data lumped into hydrological periods.

We obtained a regional estimate based on the area of flooded vegetation and open water during high and low water for a sequence of reaches along the Solimões and Amazon rivers in the central Amazon basin using data in Melack and Hess (2010). From Marañón to Gurupá, their high water area of flooded forests, woodlands, and shrubs (52,700 km^2) combined with our high water estimates of CO_2 flux, using the proportional areas of wind-sheltered and wind-exposed forest calculated for Janauacá, yields a total high water flux of 133 $\pm$ 65 Tg·C for these reaches. When extrapolated to the total high water area of flooded forests, woodlands, and shrubs for the lowland basin (630,000 km^2; Melack & Hess, 2010), the total high water flux is 1,590 $\pm$ 780 Tg·C.

4. Discussion

4.1. Diel, Seasonal, and Spatial Variability of CO_2 Concentrations and Fluxes

As we hypothesized, the WE site near a large area of open water had higher CO_2 fluxes and k values compared to the more sheltered WP site. This result is related to the increased advection, mixing, and turbulence occurring in sites near large open water areas. Daily fluxes measured in our study are higher than or similar to the few other measurements in waters within tropical and subtropical flooded forests (Table 2). This finding supports our suggestion that flooded forests have high rates of CO_2 evasion to the atmosphere and make a large contribution to regional CO_2 evasion in the Amazon basin.

While our time series data support previous studies that CO_2 concentrations and fluxes vary seasonally, the frequency of our measurements further illustrated that variability was high at each site and during each measurement period. We corroborate previous studies reporting higher CO_2 concentrations and fluxes during the high water period for Amazonian rivers (Almeida et al., 2017; Amaral et al., 2019; Devol et al., 1995; Richey et al., 1990) and floodplain lakes (Abril et al., 2014; Rudorff et al., 2011). The seasonal pattern can be explained by (i) increases in water depth that increase depth integrated respiration (Devol et al., 1995; Forsberg et al., 2017) and (ii) the extent of inundation of the floodplains. CO_2 concentrations in floodplains are positively related to the area of inundated vegetated habitats (Abril et al., 2014; Amaral et al., 2019; Borges et al., 2015) that are greater during the high water period (Melack & Hess, 2010). The vegetated habitats contribute particulate organic carbon and DOC to the floodplains that can be decomposed in situ, generating CO_2 and CH_4, buried in the sediments or transported laterally to the rivers (Engle et al., 2008; Melack & Engle, 2009; Melack & Forsberg, 2001; Richey et al., 1988, 1990). Additionally, they contribute CO_2 to floodplain waters via root respiration (Hamilton et al., 1995; Piedade, Ferreira, et al., 2010).

Day–night differences were one source of the variability but were statistically significant only for CO_2 fluxes and k_{600} at the WP site with higher mean values during the day. Wind-induced currents or internal waves within the stratified waters of the flooded forests and neighboring habitats may have transported or mixed

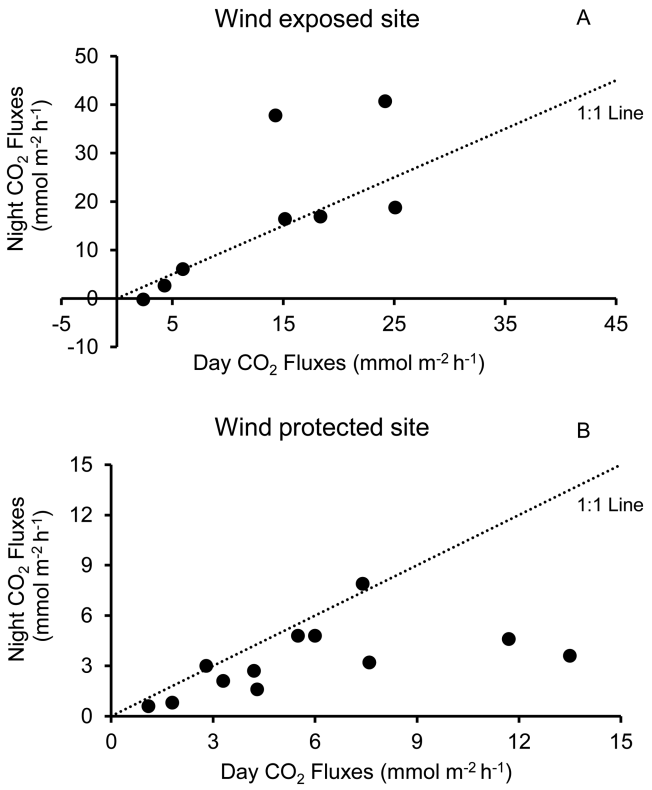

Figure 4. Mean CO_2 fluxes measured during the night versus measurements made during the day for the (a) wind-exposed and (b) wind-protected sites. Dashed lines represent the 1:1 lines.

water with elevated CO_2 concentrations into the surface waters within the flooded forest. Near-surface turbulence in the forest may have increased in the day due to advective flows generated outside the forest and higher wind speeds resulting in higher gas transfer velocities (MacIntyre et al., 2019). Values of k_{600} under these conditions will be higher than those expected from convection at night when winds are negligible. At the WE site, values were similar during the day and night except on two occasions when fluxes at night were nearly twice those in the day (Figure 4a). These occurred during high water in May and June 2015 when water depths were 5 to 7 m, depths where CO_2 did accumulate, and anoxia developed because stratification can persist. The actively mixing layer increased from 1.2 to 6 m at night, as indicative of mixing, and surface CO_2 concentrations increased (Figure 5). Fluxes increased as a result.

The variability of k_{600} was higher at the WE site as were mean values (6.7 $\pm$ 4.6 *SD*) relative to the WP site (2.3 $\pm$ 1.6 *SD*; Figure S3). The higher k_{600} values are likely associated with increases in shear in the surface waters of the flooded forest caused by wind-induced water currents from nearby open water (MacIntyre et al., 2019). Ho et al. (2018) obtained similar results in the Everglades.

Between year variability in surface water CO_2 concentrations occurred at the WP site. Values were higher in Year 1, likely because of more extensive and a longer inundation. Additionally, floating macrophytes whose decay and root respiration contributes to CO_2 in the water column (Hamilton et al., 1995; Mortillaro et al., 2016; Waichman, 1996) were present in Year 1 but not in Year 2. Advective flows can transport this water with higher gas concentration into the flooded forests. Thus, between year differences in the hydrological conditions contribute to variability.

The interannual differences have implications for understanding possible impacts of climate change in tropical floodplains. For example, extreme events are increasing in frequency in the Amazon basin (Marengo & Espinoza, 2016), and projected climate change scenarios indicate reductions in the extent of inundated areas during the low water period (Sorribas et al., 2016), similar to our observations in Year 2. Our results support a reduction in CO_2 concentrations and fluxes from flooded forests under this scenario. However, we did not measure the fluxes from exposed sediments. Evidence from other studies in flooded forests in tropical (Tathy et al., 1992) and temperate (Happell & Chanton, 1993; Pulliam, 1993) zones reports positive CO_2 fluxes from nonflooded sediments in the floodable forest. However, Dalmagro et al. (2019) reported CO_2 fluxes ingassing during flooded season and outgassing during dry season in a study in seasonally inundated forests of the Pantanal floodplain. Additional measurements from exposed sediments during the noninundated phase are needed to allow a better evaluation of the impacts of variations in inundation periods.

4.2. Inverse Relation Between CO_2 Concentrations and DO

An inverse relation between CO_2 concentrations and DO was observed in this study as in many freshwater ecosystems, including tropical floodplains along sub-Saharan African rivers (Borges et al., 2015), the Pantanal (Hamilton et al., 1995), and temperate swamp forests (Happell & Chanton, 1993). In the Pantanal wetlands, the highest CO_2 concentrations and fluxes occurred as flooding began because of decomposition of freshly inundated soil and plant organic matter (Dalmagro et al., 2018; Hamilton et al., 1997). The inverse relation between CO_2 concentrations and DO suggests that aerobic processes are important for CO_2 production. Sediment respiration (Cardoso et al., 2013), methane oxidation (Barbosa et al., 2018), and planktonic respiration (Amaral et al., 2018; Waichman, 1996; Ward et al., 2013) are all processes that consume DO and produce dissolved CO_2.

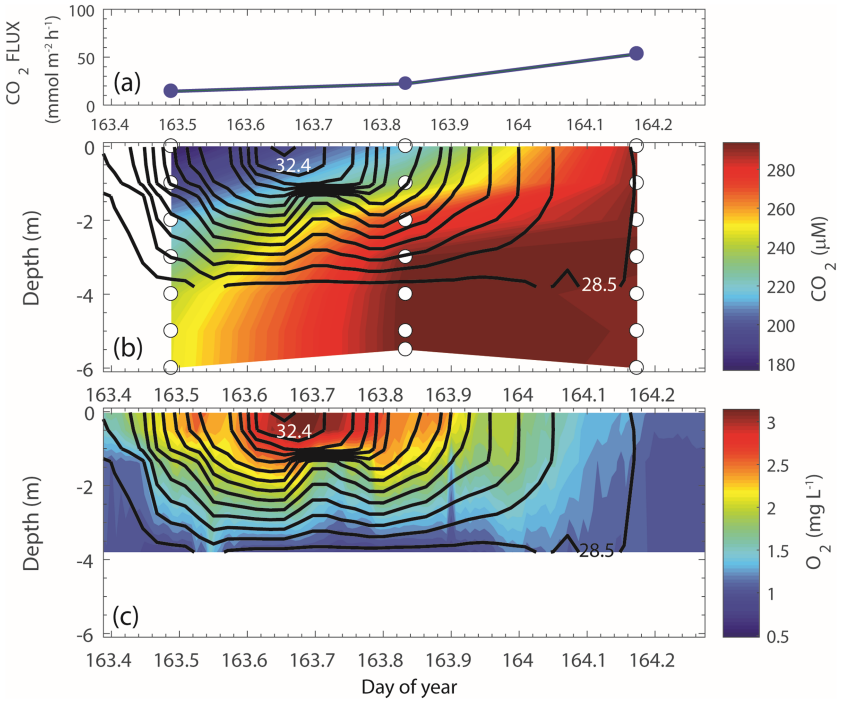

Figure 5. (a) time series of CO_2 fluxes, (b) dissolved CO_2 concentrations from discrete measurements at depths indicated by white dots, and (c) 10 min averaged time series of dissolved oxygen in the wind-exposed flooded forest in June 2015. Hourly averaged isotherms at 0.3 °C intervals are shown as black contours with maximum and minimum isotherms labelled.

More CO_2 was produced at our sites than expected by aerobic respiration within the water column (Figure 6). If aerobic respiration and CO_2 production were in balance, the excess of CO_2 (Ex-CO_2, i.e., CO_2 in the water subtracted from equilibrium CO_2 saturation) and the apparent oxygen utilization (AOU, i.e., atmospheric equilibrium O_2 solubility subtracted from the O_2 concentration measured in surface water) would follow a 1:1 line. Processes that could cause increased CO_2 production or elevated Ex-CO_2 include methanogenesis (Bartlett et al., 1988), groundwater CO_2 inputs, and root respiration within the flooded forest and associated herbaceous plants that use atmospheric CO_2 in photosynthesis and release respired CO_2 through their inundated roots (Abril et al., 2014; Abril & Borges, 2019; Melack et al., 2009; Piedade, Junk, et al., 2010). The first two processes were not likely to be important at our sites. Ex-CO_2 was not correlated with methane measured at these sites (Barbosa, 2018; $p > 0.05$, $r^2 = 0.0063$, slope = 0.0019), and the contribution of groundwater to the hydrologic balance is less than 1% in Janauacá (Bonnet et al., 2017).

The Ex-CO_2 vs AOU relation in our study is similar to the relation reported for the Solimões River and other Amazon waters (Devol et al., 1995; Richey et al., 1988). These studies suggested the importance of lateral floodplains as sites for CO_2 production and sources to the rivers. This hypothesis was examined by Abril et al. (2014), who used a one-dimensional model for CO_2 transport by the Amazon River to demonstrate that CO_2 from floodplains could be transported downstream over hundreds of kilometers. Further evidence of inputs of labile organic carbon to the rivers from floodplains is provided by measurements in the eastern Amazon by Moreira-

Table 2
Average CO_2 Diffusive Flux (FCO_2) Measured Within Flooded Forests From Different Studies

Location	Forest type	Method	FCO_2 mg C·m^{-2} d^{-1}
Amazon basin[a]	Floodplain	Chamber	343
Florida, USA[b]	Swamp	Chamber	973 ± 599
Georgia, USA[c]	Floodplain	Chamber	115 − 1270
Congo basin[d]	Floodplain	Chamber	2,640 ± 1,370
Pantanal, Brazil[e]	Floodplain	Modeled	320
Northern Australia[f]	Floodplain	Chamber	1,260 ± 1,258
Amazon basin[g]	Floodplain	Chamber	2,182 ± 2,954

[a]Devol et al. (1988). Mean value calculated from nine measurements made during the high-water period. [b]Happell and Chanton (1993). Mean value calculated from single daytime measurements once a month for 1 year. [c]Pulliam (1993). Range of mean daily fluxes obtained from ten transects with three measurements done at a monthly frequency for a 2-year period. [d]Tathy et al. (1992). Mean value from eleven daily measurements made in flooded forests. [e]Dalmagro et al. (2018). Mean value obtained using 40 measurements of surface CO_2 water concentrations and a wind-based equation during the flooded season (March to June). [f]Bass et al. (2014). Mean value obtained from seven sites with daily replicate measurements done eight times during the flood season (February to May). [g]This study. Mean value from two sites with multiple measurements over diel cycles in 12 monthly campaigns distributed through two hydrological years when the forest sites were flooded and accessible.

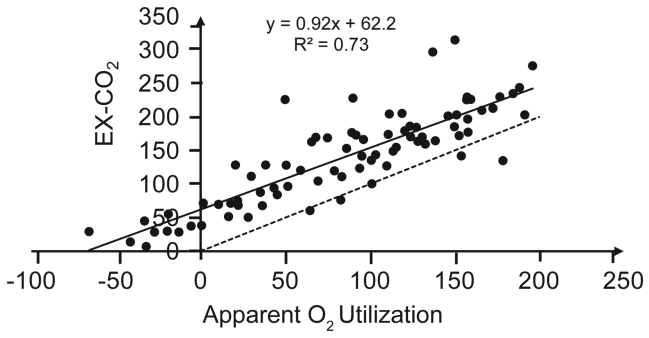

Figure 6. Excess of CO_2 as function of apparent oxygen utilization (AOU) in μM, calculated for near-surface waters of inundated forests. Dashed line is the 1:1 line, and solid black line is the regression line.

Turcq et al. (2013). Moreover, Richey et al. (1990) suggested that aquatic and terrestrial macrophytes and flooded forests in floodplains were likely sources of labile organic C for the mainstem river.

We also observed negative AOU values that represent times when photosynthetic oxygen production exceeded respiration within the flooded forests. The negative AOU values occurred when water depths were 1.5 to 3.5 m and DO concentrations were 7.4 to 9.3 mg L^{-1} in the flooded forest sites. These concentrations were similar to those observed in nearby open water.

4.3. Implications for the Regional C Budget and Other Forested Wetlands

To our knowledge, we provide the first multiseason study of CO_2 concentrations and fluxes in flooded forests for the Amazon basin. The one prior study reported nine CO_2 measurements made in July and August 1985 in flooded forests fringing open water areas, similar to our WE site (Devol et al., 1988). The range of values in that study, 466–2,400 mg C·m^{-2} d^{-1}, is lower than the range, 3,706–15,867 mg C·m^{-2} d^{-1}, (n = 19) observed during a comparable period of our study, high water at the WE site.

Mean daily fluxes measured in our study (2,182 ± 2,954 *SD* mg C·m^{-2} d^{-1}) are higher than or similar to the few other measurements in waters within tropical and subtropical flooded forests (Table 2). The low CO_2 efflux reported by Dalmagro et al. (2018) is likely related to their use of a wind-based equation to estimate the CO_2 fluxes. While wind speeds in flooded forest sites are low, other processes can increase fluxes, as noted above and in MacIntyre et al. (2019). The large range in our study indicates the need for a sampling over diel cycles on a seasonal basis (Table 2).

Seasonally inundated and riparian forests are the main aquatic habitat within the lowland Amazon basin (Hess et al., 2015; Junk et al., 2010; Melack & Hess, 2010). Most of these forests are likely to be more similar to our WP site, as the open water areas in the lowland Amazon basin corresponds to only 8% of the total basin area (Melack & Hess, 2010). Inundated forests vary in distribution and floristic composition depending on fluvial geomorphology, flooding regimes, and soil and water qualities (Junk et al., 2010). CO_2 fluxes among these forest types are likely to vary.

We report a total high water flux, integrated to the area of flooded forests, woodlands, and shrubs during this period, for the lowland Amazon of 1,590 ± 777 Tg C. For comparison, Melack and Hess's (2010) estimate of open water in rivers and lakes at high water (64,700 km^2) and the mean CO_2 fluxes reported mainly for rivers by Amaral et al. (2019; 4.7 g C·m^{-2} d^{-1}) and Richey et al. (1990; 5.2 g C·m^{-2} d^{-1}) yields a total high water flux from open water of 320 Tg C. Since fluxes from lakes are often less than from rivers (Melack, 2016; Polsenaere et al., 2013; Rudorff et al., 2011), this estimate for open water is likely high. At low water, Melack and Hess (2010) estimated that flooded forests, woodlands, and shrubs covered 17,270 km^2 of the mainstem reaches. To provide annual estimates will require time series of inundated habitats derived from hydrological models and remote sensing analysis, such as those done by Arnesen et al. (2013) and Ferreira-Ferreira et al. (2015) that map the duration of inundation of flooded forests distributed throughout the Amazon basin. Measurements of CO_2 fluxes from other types of flooded forests are also essential.

Regional estimates of CO_2 fluxes offered by Richey et al. (2002) and Melack (2016) did not include data from flooded forests. Melack's (2016) estimate for floodplains and wetland habitats used an average pCO_2 value (335 μM; 10,900 μatm) from Richey et al. (2002) and k_{600} of 12 cm hr^{-1} from studies in lakes. Our lower k_{600} values for flooded forests, a large component of floodplain and wetland habitats, clearly indicate a lower overall flux than suggested in Melack (2016). Richey et al. (2002) selected a k_{600} of 2.7 cm hr^{-1} as a conservative value for floodplains and lakes. Though low for lakes, this value is similar to our k_{600} values for sheltered flooded forests. As a consequence, their regional estimate, if expressed as mmol C·m^{-2} d^{-1} (189 ± 55), is similar to our mean value (182 ± 247) for flooded forests on the Janauacá floodplain. These new estimates highlight the importance of flooded forests for the carbon budget of the Amazon basin and the need for more studies in these aquatic habitats.

Seasonally inundated forests in the Amazon and elsewhere occur in an aquatic–terrestrial transition zone that includes other aquatic habitats such as open waters and macrophytes. Integration of C fluxes in the ATTZ is challenging, as the aquatic habitats are interconnected and interact with each other. For comparison, we contrast our mean CO_2 evasion with an estimate of net primary production (NPP) of 1,150 Mg C·km^{-2}yr^{-1} for flooded forests in the central Amazon basin (Melack & Forsberg, 2001; Worbes, 1997). This rate is based on 30% of the live wood increment, fine litter, and large woody detritus inputs to the aquatic system. Our mean CO_2 evasion (590 Mg C·km^{-2}yr^{-1}) is about half of the NPP estimate, considering that these forests remain flooded for 270 days a year. The excess of C inputs from NPP corroborates findings by other studies that argue for the mixed C sources to supply CO_2 evasion rates in open waters of the Amazon basin (Engle et al., 2008; Melack & Forsberg, 2001; Quay et al., 1992; Ward et al., 2013, 2016).

We suggest that C studies in aquatic habitats of ATTZ integrate C fluxes by weighting their relative areal coverage in the floodplain. This practice will avoid overrepresentation of recent floodplain CO_2 flux estimates (e.g., de Rasera et al., 2013; Melack, 2016) that are based mainly on data obtained from open water habitats but extrapolated to areas that encompass other aquatic habitats with different characteristics and typically lower emissions, such as flooded forests and floating macrophytes. Future studies in flooded forests should aim to improve estimates of tree stem CO_2 fluxes as well as fluxes from soil when these forests are not inundated.

Abril and Borges (2019) review the conceptual framework of carbon fluxes in the terrestrial aquatic continuum and highlight the need for including flooded land as a component in this continuum. They propose that C fluxes from flooded lands should be treated as a transport term between upland and inland waters. An example of their conceptual framework is provided by an organic carbon budget developed by Melack and Engle (2009) for an Amazon floodplain lake. More C budgets studies in flooded lands are needed as the basis for modeling studies as well as to provide correct comparisons between the terrestrial and aquatic C fluxes.

The results from our study demonstrate the importance of combining gas measurements with meteorological and limnological information to understand CO_2 fluxes in flooded forests. Additional direct measurements of k and studies of the mechanisms that generate turbulence and effects on k_{600} under low wind speed conditions are needed. We recommend that further studies include measurements throughout the day and night. The contrasting k and CO_2 fluxes values observed in sheltered flooded forests versus wind-exposed forests should be considered in the integration of CO_2 fluxes in forested wetlands.

Data Statement

Data were deposited in the KNB data repository operated by NCEAS and assigned a DOI:10.5063/F1CR5RPD (https://doi.org/10.5063/F1CR5RPD.)

No authors have financial conflicts of interest.

Acknowledgments
This work was supported by the Conselho Nacional de Pesquisa e Desenvolvimento—Ministério da Ciência Tecnologia (CNPq/MCTI); CNPq/LBA-Edital.68/2013, processo 458036/2013-7, CNPq-Universal processo.482004/2012-6. Postgraduate scholarships were provided to JHFA and by Coordenação de Aperfeiçomento de Pessoal de Nível Superior (CAPES) and CNPq. PMB and JHFA are thankful to CAPES for the grant "Programa de Doutorado Sanduíche no Exterior"—88881.135203/2016-0100 and 88881.134945/2016-0100 respectively. During manuscript, preparation support was provided to JHFA and PMB by NASA grant NNX17AK49G. JMM received support from National Aeronautics and Space Administration (NASA), the US Department of Energy (contract no. DE-0010620), the US National Science Foundation (NSF DEB grant 1753856), and a Fulbright fellowship. The authors thank for the logistical support of INPA, João B. Rocha for the field support, and Lúcia Silva for offering the floating house as a research base. We thank Michaela Melo and Jonismar S. da Silva for help in field campaigns, and Nicholas Marino for contributions regarding statistical analyses and Alberto Vieira Borges for comments in an early version of the manuscript.

References

Abril, G., & Borges, A. V. (2019). Ideas and perspectives: Carbon leaks from flooded land: do we need to replumb the inland water active pipe? *Biogeosciences*, *16*(3), 769–784. https://doi.org/10.5194/bg-16-769-2019

Abril, G., Martinez, J. M., Artigas, L. F., Moreira-Turcq, P., Benedetti, M. F., Vidal, L., et al. (2014). Amazon River carbon dioxide outgassing fuelled by wetlands. *Nature*, *505*(7483), 395–398. https://doi.org/10.1038/nature12797

Alin, S. R., Rasera, M. F. F. L., Salimon, C. I., Richey, J. E., Holtgrieve, G. W., Krusche, A. V., & Snidvongs, A. (2011). Physical controls on carbon dioxide transfer velocity and flux in low-gradient river systems and implications for regional carbon budgets. *Journal of Geophysical Research*, *116*, G01009. https://doi.org/10.1029/2010JG001398

Almeida, R. M., Pacheco, F. S., Barros, N., Rosi, E., & Roland, F. (2017). Extreme floods increase CO $_2$ outgassing from a large Amazonian river. *Limnology and Oceanography*, *62*(3), 989–999. https://doi.org/10.1002/lno.10480

Amaral, J. H. F., Borges, A. V., Melack, J. M., Sarmento, H., Barbosa, P. M., Kasper, D., et al. (2018). Influence of plankton metabolism and mixing depth on CO_2 dynamics in an Amazon floodplain lake. *Science of the Total Environment*, *630*, 1381–1393. https://doi.org/10.1016/j.scitotenv.2018.02.331

Amaral, J. H. F., Farjalla, V. F., Melack, J. M., Kasper, D., Scofield, V., Barbosa, P. M., & Forsberg, B. R. (2019). Seasonal and spatial variability of CO_2 in aquatic environments of the central lowland Amazon basin. *Biogeochemistry*, *143*(1), 133–149. https://doi.org/10.1007/s10533-019-00554-9

Arnesen, A. S., Silva, T. S. F., Hess, L. L., Novo, E. M. L. M., Rudorff, C. M., Chapman, B. D., & McDonald, K. C. (2013). Monitoring flood extent in the lower Amazon River floodplain using ALOS/PALSAR ScanSAR images. *Remote Sensing of Environment*, *130*, 51–61. https://dx.doi.org/10.1016/j.rse.2012.10.035

Barbosa, P. M. (2018). Dinâmica do metano em um lago de planície de inundação tropical (Doctoral dissertation). Retrieved from [PPGEcologia UFRJ]. (http://www.ppge.ufrj.br/teses). Rio de Janeiro, RJ, Brazil: Universidade Federal do Rio de Janeiro.

Barbosa, P. M., Farjalla, V. F., Melack, J. M., Amaral, J. H. F., da Silva, J. S., & Forsberg, B. R. (2018). High rates of methane oxidation in an Amazon floodplain lake. *Biogeochemistry*, *137*(3), 351–365. https://doi.org/10.1007/s10533-018-0425-2

Barbosa, P. M., Melack, J. M., Farjalla, V. F., Amaral, J. H. F., Scofield, V., & Forsberg, B. R. (2016). Diffusive methane fluxes from Negro, Solimões and Madeira rivers and fringing lakes in the Amazon basin. *Limnology and Oceanography*, *61*(S1), S221–S237. https://doi.org/10.1002/lno.10358

Bartlett, K. B., Crill, P. M., Sebacher, D. I., Harriss, R. C., Wilson, J. O., & Melack, J. M. (1988). Methane flux from the central Amazonian floodplain. *Journal of Geophysical Research*, *93*(D2), 1571–1582. https://doi.org/10.1029/JD093iD02p01571

Barton, K., & Barton, M. K. (2018). Package 'MuMIn'. *Version*, 1, 18.

Bass, A., O'Grady, D., Leblanc, M., Tweed, S., Nelson, P., & Bird, M. (2014). Carbon dioxide and methane emissions from a wet/dry tropical floodplain in Northern Australia. *Wetlands*, *34*(3), 619–627. https://doi.org/10.1007/s13157-014-0522-5

Bonnet, M. P., Pinel, S., Garnier, J., Bois, J., Resende Boaventura, G., Seyler, P., & Motta Marques, D. (2017). Amazonian floodplain water balance based on modelling and analyses of hydrologic and electrical conductivity data. *Hydrological Processes*, *31*(9), 1702–1718. https://doi.org/10.1002/hyp.11138

Borges, A. V., Darchambeau, F., Teodoru, C. R., Marwick, T. R., Tamooh, F., Geeraert, N., et al. (2015). Globally significant greenhouse-gas emissions from African inland waters. *Nature Geoscience*, *8*(8), 637–642. https://doi.org/10.1038/ngeo2486

Burnham, K. P., & Anderson, D. R. (2002). *Model selection and multimodel inference: a practical information-theoretic approach*, (2nd ed.). New York: Springer.

Cardoso, S. J., Vidal, L. O., Mendonça, R. F., Tranvik, L. J., Sobek, S., & Fábio, R. (2013). Spatial variation of sediment mineralization supports differential CO_2 emissions from a tropical hydroelectric reservoir. *Frontiers in Microbiology*, *4*. https://doi.org/10.3389/fmicb.2013.00101

Cole, J. J., Prairie, Y. T., Caraco, N. F., McDowell, W. H., Tranvik, L. J., Striegl, R. G., et al. (2007). Plumbing the global carbon cycle: Integrating inland waters into the terrestrial carbon budget. *Ecosystems*, *10*(1), 172–185. https://doi.org/10.1007/s10021-006-9013-8

Dalmagro, H. J., Lathuillière, M. J., Hawthorne, I., Morais, D. D., Pinto, O. B. Jr., Couto, E. G., & Johnson, M. S. (2018). Carbon biogeochemistry of a flooded Pantanal forest over three annual flood cycles. *Biogeochemistry*, *139*(1), 1–18. https://doi.org/10.1007/s10533-018-0450-1

Dalmagro, H. J., Zanella de Arruda, P. H., Vourlitis, G. L., Lathuillière, M. J., de Nogueira, S., Couto, E. G., & Johnson, M. S. (2019). Radiative forcing of methane fluxes offsets net carbon dioxide uptake for a tropical flooded forest. *Global Change Biology*, *25*(6), 1967–1981. https://doi.org/10.1111/gcb.14615

de Rasera, F. M., Krusche, A. V., Richey, J. E., Ballester, M. V. R., & Victória, R. L. (2013). Spatial and temporal variability of pCO_2 and CO_2 efflux in seven Amazonian Rivers. *Biogeochemistry*, *116*(1–3), 241–259. https://doi.org/10.1007/s10533-013-9854-0

Devol, A. H., Forsberg, B. R., Richey, J. E., & Pimentel, T. P. (1995). Seasonal variation in chemical distributions in the Amazon (Solimões) River: A multiyear time series. *Global Biogeochemical Cycles*, *9*(3), 307–328. https://doi.org/10.1029/95GB01145

Devol, A. H., Richey, J. E., Clark, W. A., King, S. L., & Martinelli, L. A. (1988). Methane emissions to the troposphere from the Amazon floodplain. *Journal of Geophysical Research*, *93*(D2), 1583–1592. https://doi.org/10.1029/JD093iD02p01583

Dixon, P. M. (1993). The bootstrap and the jackknife: Describing the precision of ecological indices. In S. M. Scheiner, & J. Gurevitch (Eds.), *Design and analysis of ecological experiments* (pp. 290–318). Oxford: Oxford University Press.

Engle, D. L., Melack, J. M., Doyle, R. D., & Fisher, T. R. (2008). High rates of net primary productivity and turnover for floating grasses on the Amazon floodplain: Implications for aquatic respiration and regional CO_2 flux. *Global Change Biology*, *14*, 369–381. https://doi.org/10.1111/j.1365-2486.2007.01481.x

Ferreira-Ferreira, J., Silva, T. S. F., Streher, A. S., Affonso, A. G., Furtado, L. F. A., Forsberg, B. R., et al. (2015). Combining ALOS/PALSAR derived vegetation structure and inundation patterns to characterize major vegetation types in the Mamirauá Sustainable Development Reserve, Central Amazon Floodplain, Brazil. *Wetlands Ecology and Management*, *23*, 41–59. https://doi.org/10.1007/s11273-014-9359-1

Forsberg, B. R., Melack, J. M., Richey, J. E., & Pimentel, T. P. (2017). Regional and seasonal variability in planktonic photosynthesis and planktonic community respiration in Amazon floodplain lakes. *Hydrobiologia*, *800*(1), 187–206. https://doi.org/10.1007/s10750-017-3222-3

Fox, J., Weisberg, S., Adler, D., Bates, D., Baud-Bovy, G., Ellison, S., et al. (2012). *Package 'car'*. Vienna: R Foundation for Statistical Computing.

Frankignoulle, M., Borges, A., & Biondo, R. (2001). A new design of equilibrator to monitor carbon dioxide in highly dynamic and turbid environments. *Water Research*, *35*(5), 1344–1347. https://doi.org/10.1016/S0043-1354(00)00369-9

Galipaud, M., Gillingham, M. A. F., David, M., & Dechaume-Moncharmont, F.-X. (2014). Ecologists overestimate the importance of predictor variables in model averaging: A plea for cautious interpretations. *Methods in Ecology and Evolution*, *5*(10), 983–991. https://doi.org/10.1111/2041-210X.12251

Gao, B. (1996). NDWI—A normalized difference water index for remote sensing of vegetation liquid water from space. *Remote Sensing of Environment*, *58*(3), 257–266.

Grueber, C. E., Nakagawa, S., Laws, R. J., & Jamieson, I. G. (2011). Multimodel inference in ecology and evolution: Challenges and solutions: Multimodel inference. *Journal of Evolutionary Biology*, *24*(4), 699–711. https://doi.org/10.1111/j.1420-9101.2010.02210.x

Hamilton, S. K., Sippel, S. J., & Melack, J. M. (1995). Oxygen depletion and carbon dioxide and methane production in waters of the Pantanal wetland of Brazil. *Biogeochemistry*, *30*(2), 115–141. https://doi.org/10.1007/BF00002727

Hamilton, S. K., Sippel, S. J., Calheiros, D. F., & Melack, J. M. (1997). An anoxic event and other biogeochemical effects of the Pantanal wetland on the Paraguay River. *Limnology and Oceanography*, *42*(2), 257–272. https://doi.org/10.4319/lo.1997.42.2.0257

Happell, J. D., & Chanton, J. P. (1993). Carbon remineralization in a north Florida swamp forest: Effects of water level on the pathways and rates of soil organic matter decomposition. *Global Biogeochemical Cycles*, *7*(3), 475–490. https://doi.org/10.1029/93GB00876

Hess, L. L., Melack, J. M., Affonso, A. G., Barbosa, C., Gastil-Buhl, M., & Novo, E. M. L. M. (2015). Wetlands of the lowland Amazon basin: Extent, vegetative cover, and dual-season inundated area as mapped with JERS-1 synthetic perture radar. *Wetlands*, *35*(4), 745–756. https://doi.org/10.1007/s13157-015-0666-y

Ho, D. T., Engel, V. C., Ferrón, S., Hickman, B., Choi, J., & Harvey, J. W. (2018). On factors influencing air-water gas exchange in emergent wetlands. *Journal of Geophysical Research: Biogeosciences*, *123*, 178–192. https://doi.org/10.1002/2017JG004299

Junk, W. J., Bayley, P. B., & Sparks, R. E. (1989). The flood pulse concept in river-floodplain systems. *Canadian Special Publication of Fisheries and Aquatic Sciences*, *106*(1), 110–127.

Junk, W. J., Piedade, M., Wittman, F., Schöngart, J., & Parolin, P. (Eds) (2010). *Amazonian floodplain forests: ecophysiology, biodiversity and sustainable management*. Dordrecht [Netherlands]; New York: Springer.

Kasper, D., Amaral, J. H. F., & Forsberg, B. R. (2018). The effect of filter type and porosity on total suspended sediment determinations. *Analytical Methods*, *10*, 5532–5539. https://doi.org/10.1039/C8AY02134A

Kemenes, A., Forsberg, B. R., & Melack, J. M. (2011). CO_2 emissions from a tropical hydroelectric reservoir (Balbina, Brazil). *Journal of Geophysical Research*, *116*, G03004. https://doi.org/10.1029/2010JG001465

Lehner, B., & Döll, P. (2004). Development and validation of a global database of lakes, reservoirs and wetlands. *Journal of Hydrology*, *296*(1–4), 1–22. https://doi.org/10.1016/j.jhydrol.2004.03.028

MacIntyre, S., Amaral, J. H. F., Barbosa, P. M., Cortés, A., Forsberg, B. R., & Melack, J. M. (2019). Turbulence and gas transfer velocities in sheltered flooded forests of the Amazon basin. *Geophysical Research Letters*, *46*, 9628–9636. https://doi.org/10.1029/2019GL083948

MacIntyre, S., Crowe, A. T., Cortés, A., & Arneborg, L. (2018). Turbulence in a small arctic pond. *Limnology and Oceanography*, *63*(6), 2337–2358. https://doi.org/10.1002/lno.10941

MacIntyre, S., & Melack, J. M. (1995). Vertical and horizontal transport in lakes: Linking littoral, benthic, and pelagic habitats. *Journal of the North American Benthological Society*, *14*(4), 599–615. https://doi.org/10.2307/1467544

MacIntyre, S., Romero, J. R., & Kling, G. W. (2002). Spatial-temporal variability in surface layer deepening and lateral advection in an embayment of Lake Victoria, East Africa. *Limnology and Oceanography*, *47*(3), 656–671. https://doi.org/10.4319/lo.2002.47.3.0656

MacIntyre, S., Wanninkhof, R., & Chanton, J. (1995). Trace gas exchange across the air-water interface in freshwater and coastal marine environments. Chapter 3. In P. Matson, & R. Harriss (Eds.), *Biogenic Trace Gases: Measuring Emissions from Soil and Water* (pp. 52–97). Cambridge, Mass: Blackwell.

Marengo, J. A., & Espinoza, J. C. (2016). Extreme seasonal droughts and floods in Amazonia: Causes, trends and impacts. *International Journal of Climatology*, *36*(3), 1033–1050. https://doi.org/10.1002/joc.4420

Melack, J. M. (2016). Aquatic Ecosystems. In L. Nagy, B. R. Forsberg, & P. Artaxo (Eds.), *Interactions between biosphere, atmosphere and human land use in the amazon basin* (pp. 119–148). Berlin, Heidelberg: Springer Berlin Heidelberg. https://doi.org/10.1007/978-3-662-49902-3_7

Melack, J. M., & Engle, D. (2009). An organic carbon budget for an Amazon floodplain lake. *Intenationale Vereinigung für Theoretische und Angewandte Limnologie: Verhandlungen*, *30*(8), 1179–1182. https://doi.org/10.1080/03680770.2009.11923906

Melack, J. M., & Forsberg, B. R. (2001). Biogeochemistry of Amazon floodplain. In M. E. McClain, R. L. Victoria, & J. E. Richey (Eds.), *The Biogeochemistry of the Amazon Basin and its Role in a Changing World* (pp. 235–276). New York, NY, USA: Oxford University Press.

Melack, J. M., & Hess, L. L. (2010). Remote sensing of the distribution and extent of wetlands in the Amazon basin. In W. J. Junk, M. T. F. Piedade, F. Wittmann, J. Schöngart, & P. Parolin (Eds.), *Amazonian Floodplain Forests* (pp. 43–59). Dordrecht: Springer Netherlands. https://doi.org/10.1007/978-90-481-8725-6_3

Melack, J. M., Hess, L. L., Gastil, M., Forsberg, B. R., Hamilton, S. K., Lima, I. B. T., & Novo, E. M. L. M. (2004). Regionalization of methane emissions in the Amazon Basin with microwave remote sensing. *Global Change Biology*, *10*(5), 530–544. https://doi.org/10.1111/j.1365-2486.2004.00763.x

Melack, J. M., Novo, E. M. L. M., Forsberg, B. R., Piedade, M. T. F., & Maurice, L. (2009). In M. Keller, M. Bustamante, J. Gash, & P. Silva Dias (Eds.), *Floodplain ecosystem processes*, *Geophysical Monograph Series* (Vol. 186, pp. 525–541). Washington, D. C.: American Geophysical Union. https://doi.org/10.1029/2008GM000721

Moreira-Turcq, P., Bonnet, M. P., Amorim, M., Bernardes, M., Lagane, C., Maurice, L., et al. (2013). Seasonal variability in concentration, composition, age, and fluxes of particulate organic carbon exchanged between the floodplain and Amazon River. *Global Biogeochemical Cycles*, *27*, 119–130. https://doi.org/10.1002/gbc.20022

Mortillaro, J. M., Passarelli, C., Abril, G., Hubas, C., Alberic, P., Artigas, L. F., et al. (2016). The fate of C4 and C3 macrophyte carbon in central Amazon floodplain waters: Insights from a batch experiment. *Limnologica*, *59*, 90–98. https://doi.org/10.1016/j.limno.2016.03.008

Pangala, S. R., Enrich-Prast, A., Basso, L. S., Peixoto, R. B., Bastviken, D., Hornibrook, E. R. C., et al. (2017). Large emissions from floodplain trees close the Amazon methane budget. *Nature*, *552*(7684), 230–234. https://doi.org/10.1038/nature24639

Parolin, P., Wittmann, F., & Schöngart, J. (2010). Tree phenology in Amazonian floodplain forests. In W. J. Junk, M. T. F. Piedade, F. Wittmann, J. Schöngart, & P. Parolin (Eds.), *Amazonian Floodplain Forests* (pp. 106–126). Dordrecht: Springer Netherlands. https://doi.org/10.1007/978-90-481-8725-6_5

Piedade, M. T. F., Ferreira, C. S., Oliveira Wittmann, A., Buckeridge, M., & Parolin, P. (2010). Biochemistry of Amazonian floodplain trees. In W. J. Junk, M. T. F. Piedade, F. Wittmann, J. Schöngart, & P. Parolin (Eds.), *Amazonian Floodplain Forests* (pp. 127–139). Dordrecht: Springer Netherlands. https://doi.org/10.1007/978-90-481-8725-6_6

Piedade, M. T. F., Junk, W., DÂngelo, S. A., Wittmann, F., Schöngart, J., Barbosa, K. M. . N., & Lopes, A. (2010). Aquatic herbaceous plants of the Amazon floodplains: State of the art and research needed. *Acta Limnologica Brasiliensia*, *22*(02), 165–178. https://doi.org/10.4322/actalb.02202006

Pinel, S., Bonnet, M.-P., Santos Da Silva, J., Moreira, D., Calmant, S., Satgé, F., & Seyler, F. (2015). Correction of interferometric and vegetation biases in the SRTMGL1 spaceborne DEM with hydrological conditioning towards improved hydrodynamics modeling in the Amazon basin. *Remote Sensing*, *7*(12), 16,108–16,130. https://doi.org/10.3390/rs71215822

Poindexter, C. M., Baldocchi, D. D., Matthes, J. H., Knox, S. H., & Variano, E. A. (2016). The contribution of an overlooked transport process to a wetland's methane emissions. *Geophysical Research Letters*, *43*, 6276–6284. https://doi.org/10.1002/2016GL068782

Polsenaere, P., Deborde, J., Detandt, G., Vidal, L. O., Pérez, M. A. P., Marieu, V., & Abril, G. (2013). Thermal enhancement of gas transfer velocity of CO_2 in an Amazon floodplain lake revealed by eddy covariance measurements. *Geophysical Research Letters*, *40*, 1734–1740. https://doi.org/10.1002/grl.50291

Pulliam, W. M. (1993). Carbon dioxide and methane exports from a southeastern floodplain swamp. *Ecological Monographs*, *63*(1), 29–53. https://doi.org/10.2307/2937122

Quay, P. D., Wilbur, D., Richey, J. E., Hedges, J. I., Devol, A. H., & Victoria, R. (1992). Carbon cycling in the Amazon River: Implications from the ^{13}C compositions of particles and solutes. *Limnology and Oceanography*, *37*(4), 857–871. https://doi.org/10.4319/lo.1992.37.4.0857

Raymond, P. A., Hartmann, J., Lauerwald, R., Sobek, S., McDonald, C., Hoover, M., et al. (2013). Global carbon dioxide emissions from inland waters. *Nature*, *503*(7476), 355–359. https://doi.org/10.1038/nature12760

Richey, J. E., Devol, A. H., Wofsy, S. C., Victoria, R., & Riberio, M. N. G. (1988). Biogenic gases and the oxidation and reduction of carbon in Amazon River and floodplain waters: Amazon dissolved gases. *Limnology and Oceanography*, *33*(4), 551–561. https://doi.org/10.4319/lo.1988.33.4.0551

Richey, J. E., Hedges, J. I., Devol, A. H., Quay, P. D., Victoria, R., Martinelli, L., & Forsberg, B. R. (1990). Biogeochemistry of carbon in the Amazon River. *Limnology and Oceanography*, *35*(2), 352–371. https://doi.org/10.4319/lo.1990.35.2.0352

Richey, J. E., Melack, J. M., Aufdenkampe, A. K., Ballester, V. M., & Hess, L. L. (2002). Outgassing from Amazonian rivers and wetlands as a large tropical source of atmospheric CO_2. *Nature*, *416*(6881), 617–620. https://doi.org/10.1038/416617a

Rudorff, C. M., Melack, J. M., MacIntyre, S., Barbosa, C. C. F., & Novo, E. M. L. M. (2011). Seasonal and spatial variability of CO_2 emission from a large floodplain lake in the lower Amazon. *Journal of Geophysical Research*, *116*, G04007. https://doi.org/10.1029/2011JG001699

Sawakuchi, H. O., Neu, V., Ward, N. D., Barros, M. . L. C., Valerio, A. M., Gagne-Maynard, W., et al. (2017). Carbon dioxide emissions along the lower Amazon River. *Frontiers in Marine Science*, *4*. https://doi.org/10.3389/fmars.2017.00076

Sorribas, M. V., Paiva, R. C. D., Melack, J. M., Bravo, J. M., Jones, C., Carvalho, L., et al. (2016). Projections of climate change effects on discharge and inundation in the Amazon basin. *Climatic Change*, *136*(3–4), 555–570. https://doi.org/10.1007/s10584-016-1640-2

Strickland, J. D., & Parsons, T. R. (1972). *A practical handbook of seawater analysis*, (p. 310). Ottawa: Fisheries Research Board of Canada.

Tathy, J. P., Cros, B., Delmas, R. A., Marenco, A., Servant, J., & Labat, M. (1992). Methane emission from flooded forest in central Africa. *Journal of Geophysical Research*, *97*(D6), 6159–6168. https://doi.org/10.1029/90JD02555

Tedford, E. W., MacIntyre, S., Miller, S. D., & Czikowsky, M. J. (2014). Similarity scaling of turbulence in a temperate lake during fall cooling. *Journal of Geophysical Research: Oceans*, *119*, 4689–4713. https://doi.org/10.1002/2014JC010135

Valderrama, J. C. (1981). The simultaneous analysis of total nitrogen and total phosphorus in natural waters. *Marine Chemistry*, *10*(2), 109–122. https://doi.org/10.1016/0304-4203(81)90027-X

Waichman, A. V. (1996). Autotrophic carbon sources for heterotrophic bacterioplankton in a floodplain lake of central Amazon. *Hydrobiologia*, *341*(1), 27–36. https://doi.org/10.1007/BF00012300

Wanninkhof, R. (1992). Relationship between wind speed and gas exchange over the ocean. *Journal of Geophysical Research*, *97*(C5), 7373. https://doi.org/10.1029/92JC00188

Ward, N. D., Bianchi, T. S., Sawakuchi, H. O., Gagne-Maynard, W., Cunha, A. C., Brito, D. C., et al. (2016). The reactivity of plant-derived organic matter and the potential importance of priming effects along the lower Amazon River. *Journal of Geophysical Research: Biogeosciences*, *121*, 1522–1539. https://doi.org/10.1002/2016JG003342

Ward, N. D., Keil, R. G., Medeiros, P. M., Brito, D. C., Cunha, A. C., Dittmar, T., et al. (2013). Degradation of terrestrially derived macromolecules in the Amazon River. *Nature Geoscience*, *6*(7), 530–533. https://doi.org/10.1038/ngeo1817

Weiss, R. F., & Price, B. A. (1980). Nitrous oxide solubility in water and seawater. *Marine Chemistry*, *8*(4), 347–359. https://doi.org/10.1016/0304-4203(80)90024-9

Wiesenburg, D. A., & Guinasso, N. L. (1979). Equilibrium solubilities of methane, carbon monoxide, and hydrogen in water and sea water. *Journal of Chemical & Engineering Data*, *24*(4), 356–360. https://doi.org/10.1021/je60083a006

Wittmann, F., Anhuf, D., & Funk, W. J. (2002). Tree species distribution and community structure of central Amazonian várzea forests by remote-sensing techniques. *Journal of Tropical Ecology*, *18*(6), 805–820. https://doi.org/10.1017/S0266467402002523

Wittmann, F., Schöngart, J., & Junk, W. J. (2010). Phytogeography, species diversity, community structure and dynamics of central Amazonian floodplain forests. In W. J. Junk, M. T. F. Piedade, F. Wittmann, J. Schöngart, & P. Parolin (Eds.), *Amazonian Floodplain Forests* (pp. 61–102). Dordrecht: Springer Netherlands. https://doi.org/10.1007/978-90-481-8725-6_4

Worbes, M. (1997). The forest ecosystem of the floodplains. In W. J. Junk (Ed.), *The Central Amazon Floodplain: Ecology of a Pulsing System* (pp. 223–265). Berlin, Heidelberg: Springer Berlin Heidelberg. https://doi.org/10.1007/978-3-662-03416-3_11

Worbes, M., Klinge, H., Revilla, J. D., & Martius, C. (1992). On the dynamics, floristic subdivision and geographical distribution of várzea forests in Central Amazonia. *Journal of Vegetation Science*, *3*(4), 553–564. https://doi.org/10.2307/3235812

Zappa, C. J., McGillis, W. R., Raymond, P. A., Edson, J. B., Hintsa, E. J., Zemmelink, H. J., et al. (2007). Environmental turbulent mixing controls on air-water gas exchange in marine and aquatic systems. *Geophysical Research Letters*, *34*, L10601. https://doi.org/10.1029/2006GL028790